

**THERMAL BALANCE TESTING OF THE MSAT SPACECRAFT**

**Serge Samson**  
Spar Aerospace Limited,  
Ste. Anne-de-Bellevue, Quebec, CANADA

**Elie Choueiry**  
David Florida Laboratory,  
Canadian Space Agency,  
Ottawa, Ontario, CANADA

**Kenneth Pang**  
Hughes Aircraft Corporation,  
El Segundo, California, U.S.A.

**ABSTRACT**

This paper reports on the recently completed thermal balance/thermal vacuum testing of an MSAT satellite, the first satellite to provide mobile communications service for all of continental North America. MSAT is a two-spacecraft program, using a three-axis-stabilized HUGHES HS-601 series bus as the vehicle for the Canadian-designed payload. The thermal tests performed at the Canadian Space Agency's David Florida Laboratory in Ottawa, Canada, lasted approximately 32 days.

**Background**

The infrared (IR) heating rig was designed to provide radiant heat inputs into seven spacecraft zones during thermal vacuum (TV) testing. The TV test was divided into multiple phases and began with a thermal balance cold phase, followed by a cold test phase and a hot balance phase, a hot test phase to finish, and finally a thermal cycle with continuous monitoring of the bus and payload. The spacecraft external heat fluxes were provided by IR lamp sources. To ensure flux uniformity, highly reflective baffles and IR lamp sources were used over six of the seven zones: the two Second Surface Mirror (SSM) radiators; the East and West faces; the Earth facing (Nadir); and the inside of the thrust cylinder. The Aft end panel heat fluxes were provided by a heated LN<sub>2</sub> shroud. The radiation flux intensity on the spacecraft zones from the various rig elements was measured using Monitored Background Radiometers (MBR), and compared with direct calculations and with pretest predictions.

The temperature measurement system was based on Uniform Temperature References (UTR) located inside the TV chamber such that all connectors and cabling were copper-copper. This system was devised to achieve a temperature measurement accuracy of  $\pm 1$  °C for over 850 thermocouples used in the test. A PC-based real-time data processing system (TVDPS) on a QNX operating system, provided continuous monitoring of all channels within a 30s time scan. Also, the TVDPS retrieved a telemetry stream from the Satellite Test Equipment (STE) station, and provided real-time data manipulation.

Preliminary results showed the test to be successful from both viewpoints - thermal balance and electrical testing.

## INTRODUCTION

MSAT is a three-axis-stabilized communications satellite designed to operate in a geostationary orbit over North America. The antennas and the SPAR-designed payload are integrated on a Hughes Aircraft HS-601 Bus. MSAT will be the first satellite to provide a mobile continental communication service. Two satellites are being tested. The first satellite (M1) will service Canada and will be operated by Telesat Mobile Inc. (TMI), while the second satellite (M2), owned by American Mobile Satellite Corporation (AMSC), will service United States territory. M1 and M2 respectively are planned to be launched in April and March 1995. Figure 1 shows MSAT with its receive and transmit L-Band antennas. Gain limitations inherent with mobile users have driven MSAT to offer high receive gain and high transmit power capabilities. The high power transmit feed is capable of radiating over 600 W RF in the L-Band frequency and is fed by 16 primary (and 4 redundant) High Power Amplifiers (HPAs). Ten HPAs are mounted on each of the North and the South radiators. Each HPA dissipates 120 W and when the forward repeater is operated, eight to ten HPAs dissipate simultaneously on the North and/or the South radiators. The HPA dissipation is distributed on the radiator surface using orthogonal imbedded heat pipes. The spreader heat pipes distribute the dissipation of each HPA in the Z axis orientation (aft-nadir) and header heat pipes are used to distribute the heat load between the HPAs themselves in the X axis orientation (East-West).

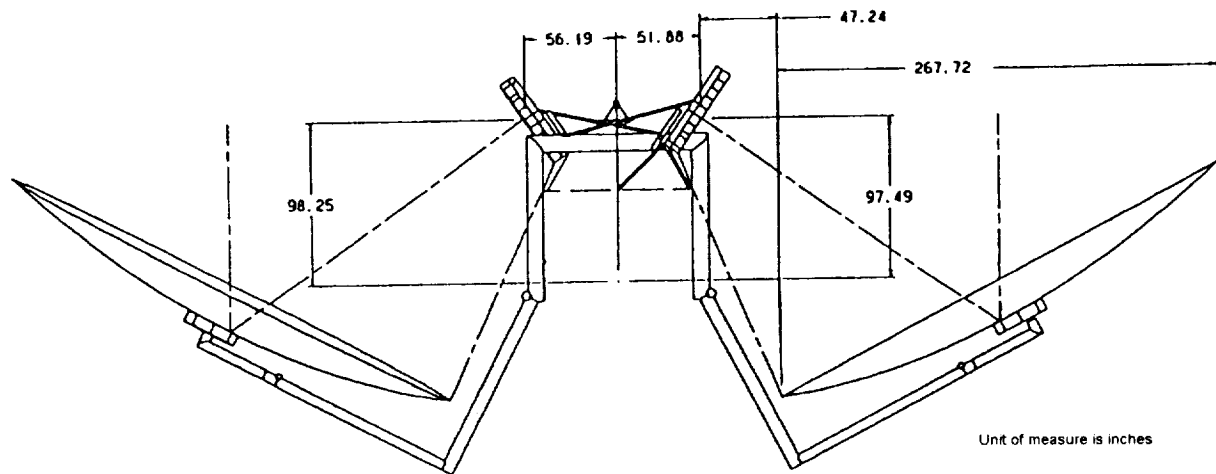


Figure 1. The MSAT satellite

Due to the MSAT program's schedule and flight hardware availability, two TV tests were performed on each satellite. Thermal balance, as well as bus and payload performance verification tests used the same setup (by using the same setup, DFL's resources were optimised and the testing time was reduced). The L-Band feeds were unavailable for the TV tests, so heated feed simulators were made to create the correct thermal boundaries for the payload. The feed thermal models were verified in a separate, thorough conductance test [Ref.1].

DFL's space simulation laboratory has integrated and tested numerous satellites and space sub-systems. Its facilities include anechoic chambers, vibration platforms, and several vacuum chambers to hold all sizes of spacecraft (7m x 11m maximum). Its anechoic chambers are used to evaluate antennas and RF payloads. Its vibration platforms are used for vibration and modal analysis to verify the structural integrity. Its vacuum chambers, in addition to providing hard vacuum testing, are also equipped for doing IR TV testing to verify the thermal design and workmanship of spacecraft. The IR TV tests are controlled and monitored in-house by the TVDPS.

## BACKGROUND

In the mid 1980's, SPAR, sponsored by DFL, developed orbital thermal simulator capability using infrared (IR) stimulation. The developed technique consisted of partitioning the appropriate spacecraft surfaces into isoflux zones each receiving an IR-equivalent radiant solar flux corresponding to a specified orbital position [Ref.4,7]. The IR fluxes were generated by IR lamps and Calrods. An IR rig structure supported the spacecraft and associated IR hardware. The use of baffles with a specular reflecting surface enhanced flux uniformity by containing flux spillover around the various zones. The total radiation input to the spacecraft surfaces was measured by specially designed Monitored Background Radiometers (MBR) [Ref.2]. The heating element configurations were determined using a software package developed by SPAR (IRFLUX) to calculate the absorbed heat flux distribution in individual zones. IRFLUX calculated both the initial heat source configurations, and the final data reduction of the measured zone flux values. The IR portion of the thermal balance test for the OLYMPUS spacecraft thermal model was carried out at DFL in the second half of January 1986, ([Ref.3] contains a detailed description of the test design). In 1990, the ANIK E (flight 1 and 2, GE Astro 5000 series) spacecraft thermal tests took place at DFL. A total of five different flux environments including eclipse, were simulated on the ANIK E spacecraft [Ref.5]. The thermal balance phase was performed first, and lasted seven days. The TV test setup enabled testing to progress directly from thermal balance to TV communications testing.

## MSAT THERMAL VACUUM TEST REQUIREMENTS

The TV tests were required to verify the Bus and Payload system performances over the qualification or acceptance temperature ranges. Spacecraft thermal balance phases were also performed to verify the satellite thermal design and correlate the thermal model. During the Bus and Payload test phases, the test heaters as well as the IR lamps are used to obtain the desired temperatures on the different subsystems.

The first TV test, identified as M2 CTV-1, was on the M2 satellite, and this test had two long performance testing phases (hot and cold), and five thermal balance phases. M2 CTV-1 lasted 32 days under vacuum. Figure 2 displays the test profile.

The second TV test, M1 CTV-1 was on the M1 satellite and consisted of Bus and Payload hot and cold testing (two phases). The next two tests (M2 CTV-2, M1 CTV-2) will consist of two system performance testing phases and some thermal balance phases.

During the thermal balance phases, the absorbed flux uniformity was required to be better than 5% over each IR zone. Every interface to the spacecraft had to be thermally isolated using a specially designed thermal blankets to minimize the heat exchange between them and the satellite. Those unwanted heat fluxes would cause inaccuracies in thermal balance correlation. Test heaters and specially designed heated multi-layer blankets (MLI) were used to maintain a temperature gradient of less than 3 °C at those interfaces between the spacecraft side temperature and the chamber side temperature.

### Thermal vacuum test design

The IR tests were performed in the 7m x 11m TV chamber. By an attachment ring, the satellite was supported horizontally inside the TV chamber. The conductive heat exchange between the spacecraft and the test structure was minimized by low-conductivity washers at their interface. The IR rig was held by the same structure (U-frame) which is supported on the tilt-adjustable support frame. This assembly sits on a large tower erected inside the TV chamber. The IR rig was installed on top of the U-frame and surrounds MSAT. Figure 3 shows the unassembled IR rig.

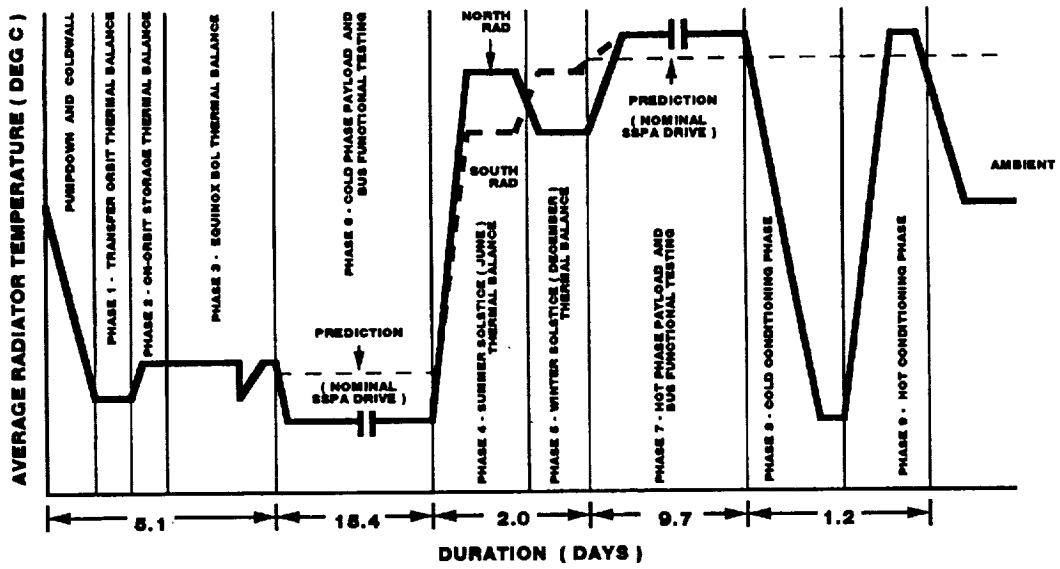


Figure 2. Test profile for M2 CTV-1 test on MSAT M2

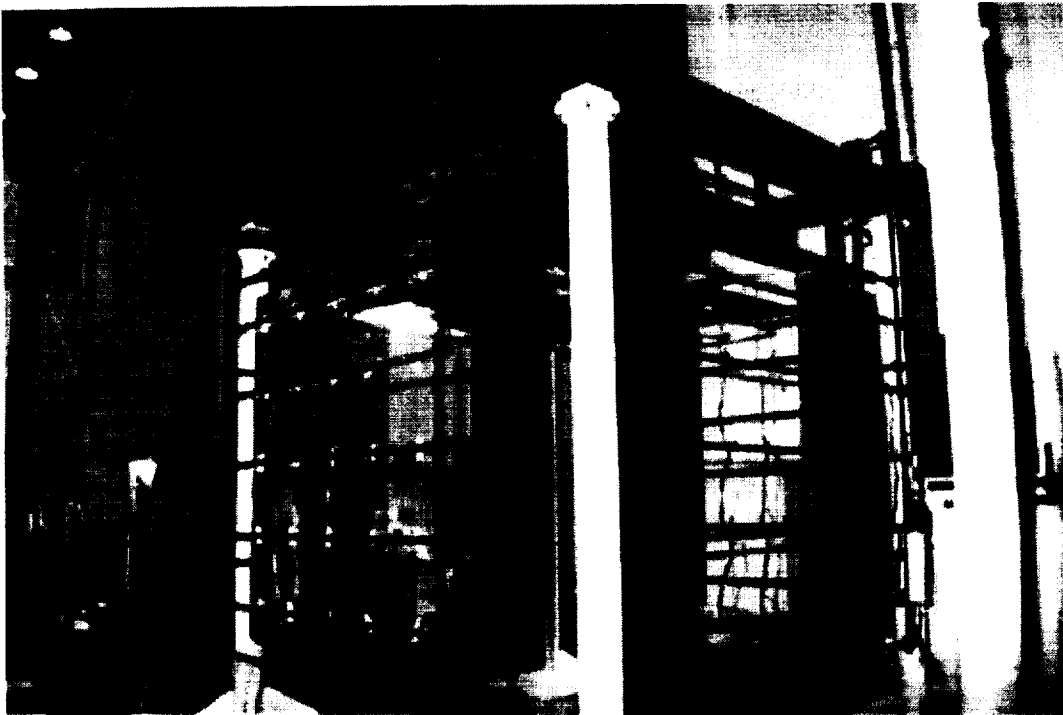


Figure 3. Unassembled IR rig assembly

ORIGINAL PAGE  
BLACK AND WHITE PHOTOGRAPH

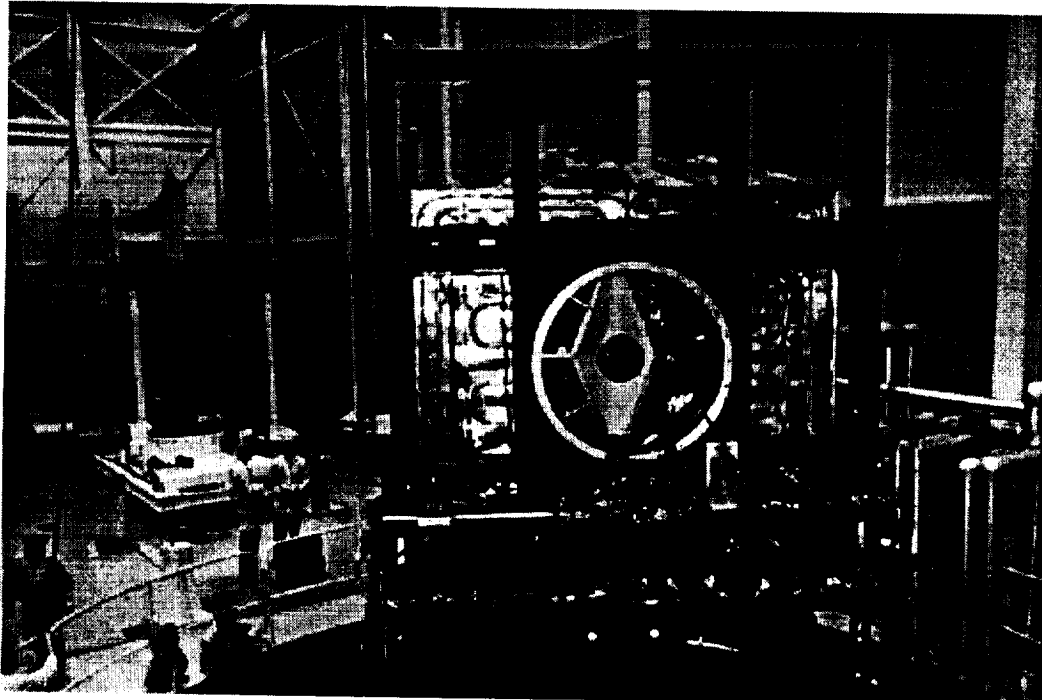


Figure 4. Complete IR assembly surrounds MSAT M2 prior to TV test

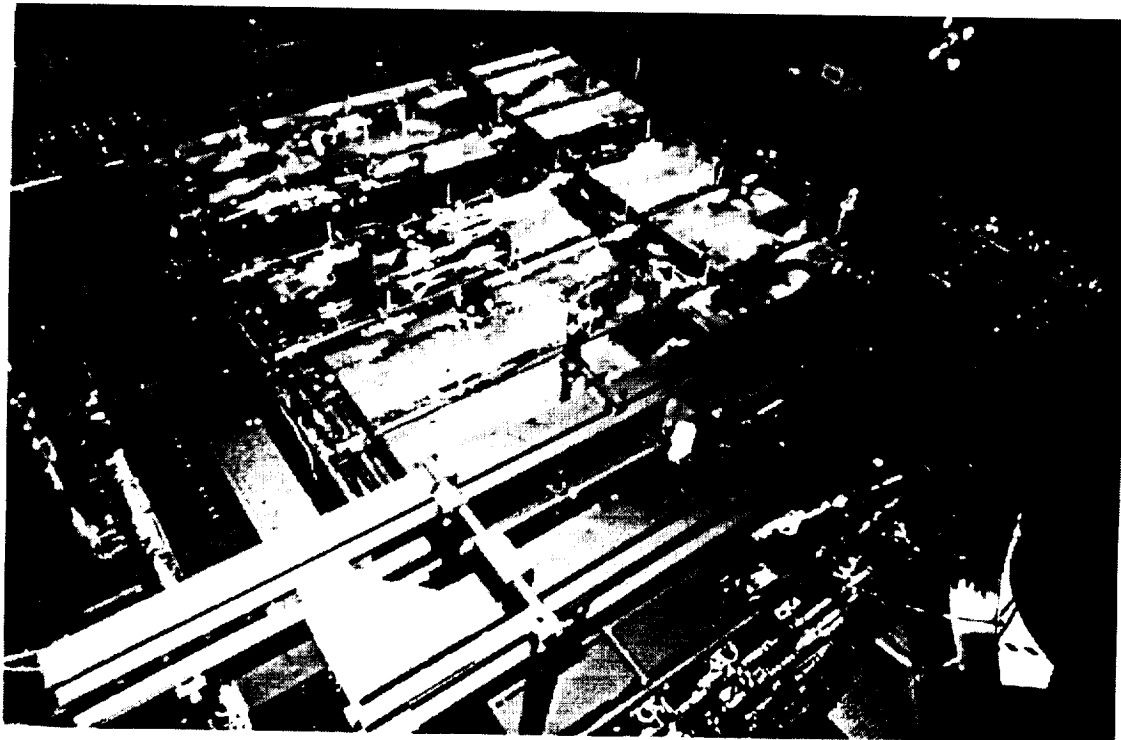


Figure 5. Complete IR assembly surrounds MSAT M2 in the 7 m x 11 m TV chamber

Figure 4 shows the complete IR assembly prior to testing, and includes the spacecraft within the IR rig. In order to prevent the satellite being affected by the IR rig and the tower structure, a high-emissivity LN<sub>2</sub> shroud is used in front of the North Radiator. The LN<sub>2</sub> shroud's high emissivity was achieved by bonding a black-painted 1" aluminum honeycomb over the LN<sub>2</sub> shroud.

The support frame is designed to maintain its horizontality to within 2 mm/m. Two leveling devices called jactuators, are located below the support frame in the -Z side of the spacecraft (AFT). The +Z end of the support frame rests on a central spherical bearing allowing for two-axis adjustments using the jactuators. The leveling can be verified with X-axis (East-West) and Z-axis (AFT-Nadir) tilt sensors. Three sensors are located on the exterior surface of each radiator panel. A level setting adjustment is performed prior to pumpdown using a high accuracy level. The tilt sensor equations are then brought to a zero degree angle value. No tilt angle adjustment have been required after pump-down of any of the four CTV tests as both the X-axis and the Z-axis stayed within  $\pm 0.05^\circ$  off-angle.

Figure 5 illustrate the complete setup prior to testing in the 7 m x 11 m TV chamber. Including pump down and recovery, a total of seven Phases were performed - five of them required heat flux inputs from the IR rig: Equinox, Summer Solstice, Winter Solstice, transfer orbit, and on-orbit storage. At the beginning of each Phase, the IR lamps were adjusted to their nominal setting. The radiometer input could then be used to refine the power setting on the IR lamp if necessary, for individual zones. The eclipse test occurred after the Equinox Phase; during this test all the IR lamps and Calrods were turned off.

Each cable or bundle interfacing with the satellite is thermally guarded so as to eliminate any conductive heat exchange between the satellite and the test hardware. Unwanted heat fluxes would cause inaccuracies in the thermal balance test correlation, so a specially-designed, heated thermal blanket was used at the different test interfaces. A resistive wire was applied to the internal layer of the guard blanket using aluminum as well as Kapton tapes. Cable thermal management was also provided using similar heated blankets. This integrated heater/blanket design significantly reduced setup time by eliminating the individual guard heater installation at each interface. Velcro and reinforced blanket material are used to recover them for use in future tests. Modular baffles and a generic IR lamp mounting structure were built for this program and remain available for use in future tests.

Distributed on the TV chamber wall around the satellite, 16 recovery lamp poles were used to recover the TV chamber and were available for emergency recoveries as well.

### IR rig design

The satellite surface was divided into seven isoflux zones. IR Research Inc.'s 500 W IR lamp sources provided heat inputs for six of these zones, namely: the North and South radiators, the East and West faces, the earth facing (Nadir), and the inside of the thrust cylinder with its LAM (liquid apogee motor). The Aft end zone was controlled with two vertical LN<sub>2</sub>-heated shrouds. As shown in Table 1, 122 IR lamps were used. IR lamp locations were computed using IRFLUX, a SPAR program developed to calculate the absorbed flux in the individual zones irradiated by IR lamps or Calrods.

IRFLUX treats each zone independently and that results in increased flexibility and reduction of execution time. The program analyzes zones either with, or without specular baffles. IRFLUX takes into account surface absorptivity variations as a function of angle of incidence and IR lamp power (radiated frequency spectrum). IRFLUX inputs are the required average absorbed flux value and the zone definitions (zone dimension, baffle locations and properties, satellite surface type). Then, IRFLUX generates the optimal IR lamp configuration and power levels required to obtain the requested average flux density. IRFLUX also provides a flux distribution matrix to produce isoflux contour plots.

Highly reflective Vacuum-Deposited Aluminum baffles delimited every zone. These baffles ensured maximum flux uniformity and contained flux spillover around various IR zones. The absorbed fluxes were accurately measured at 38 locations on the satellite's surface using 49 monitored background radiometers [Ref.3] (see Table 1).

At the beginning of each Phase, the IR lamps were adjusted to their nominal setting. The radiometer readings were compared to the IRFLUX predicted flux distribution, then appropriate corrections were made to the IR lamp power level.

Table 1. IR lamp and radiometer distribution

IR ZONE	NUMBER OF IR LAMPS	NUMBER OF RADIOMETER LOCATIONS	NUMBER OF RADIOMETERS	NEW RADIOMETERS SURFACE TYPE	OLD RADIOMETERS SURFACE TYPE
NORTH RADIATOR	20	7	9	SSM	SSM (OLYMPUS)
SOUTH RADIATOR	20	7	9	SSM	SSM (OLYMPUS)
EAST	25	5	7	CLK**	BLACK PAINT (OLYMPUS)
WEST	25	5	7	CLK**	BLACK PAINT (OLYMPUS)
NADIR	30	8	10	CLK**	BLACK PAINT (OLYMPUS)
				-	WHITE SUNSHIELD (ANIK-E)
THRUST CYLINDER	2	4	4	-	1 MIL KAPTON (ANIK E)
				WHITE PAINT	-
AFT	0*	2	3	-	1 MIL KAPTON (ANIK E)
<b>TOTAL:</b>	<b>122</b>	<b>38</b>	<b>49</b>		

\* A heated shroud was used  
 \*\* CLK : Carbon Loaded Kapton

#### Monitored background radiometers (MBRs)

The MBRs were designed and then calibrated to take a direct reading on the heat flux absorbed by a spacecraft surface. The MBRs are made of a sensing disk covered by a surface identical to the corresponding spacecraft surface and a body to form a background for the back of the sensing disk. A detailed error analysis [Ref.6] has shown that: for power levels greater than 130 W/m<sup>2</sup>, the maximum, calculated error was less than 3 %; for fluxes of 40 W/m<sup>2</sup>, it was 4.1 %; and for fluxes of 5 W/m<sup>2</sup>, it was 20 %, (for 5W/m<sup>2</sup>, this translates to less than ± 1 W/m<sup>2</sup>).

#### THERMAL VACUUM DATA PROCESSING SYSTEM (TVDPS)

DFL's Thermal Vacuum Data Processing System (TVDPS) was designed as an operator interface station to provide test or process information in formats clear and familiar to the technician or computer operator. Also, detailed historical analysis and file management functions useful to research or engineering personnel. The TVDPS's operating system is real-time, multi-tasking, multi-user, with peer-to-peer distributed network capability. Depending upon the devices attached, TVDPS communication is serial (RS-232, 422, 485) or parallel (IEEE-488). The complexity of the MSAT IR test required the setup of over 1460 input channels on the TVDPS. Channel allocations were broken down as follows: 139 miscellaneous inputs, 165 calculation channels, 210 thermal control channels, 240 telemetry channels, and 710 channels for the spacecraft and the IR rig structure.

The TVDPS can monitor, log, limit check, and graphically display data while changes occur. Update rates and throughput depend on the data acquisition unit and system configuration. Any historical (previously data logged) data may be accessed concurrently with ongoing data acquisition. Typical task switch rate is 140 μs on an 80386/20 MHz PC and 25 μs on an 80486/25 MHz PC.

Processing power in addition to the above was required to compare telemetry data with spacecraft temperatures during each phase of the test. For this purpose one of the TVDPS nodes was connected to the spacecraft telemetry system, which consisted primarily of a VMS-based DEC VAX 4000-200. An interface routine was implemented to serially receive ASCII formatted data at 9600 baud from the DEC VAX 4000-200. This information was sequentially retrieved and stored in the TVDPS internal database. Real-time or historical plots could be generated to correlate any number of activities at any time during the TV test.

## Temperature measurement system

The high accuracy of the temperature measurement system is maintained because the design of specialised feedthroughs, and the Uniform Temperature Reference (UTR) block-and-case assembly. Into each UTR, up to 30 thermocouples were plugged and this maintained a homogeneous temperature throughout all of the attachment points. Two distinct copper extension cable assemblies connect each UTR block to one TVDPS datalogger. The copper extension cable wires are connected by a 34-pin vacuum-feedthrough; two pins of which are used for connecting the common shields together. Thus the reference temperature for the thermocouples is now UTR temperature. UTR reference temperature is measured by comparing it with a 0 °C reference thermocouple which is immersed in an ice bath outside the vacuum environment.

## Thermal control system

The thermal control system has 256 microprocessor-controlled DC power supplies, each capable of delivering up to 2 kW of regulated and monitored output power into a resistive load. To minimize the consequences of hardware failure and increase the versatility of the user, the thermal control system is of a modular design. To reduce the size of the equipment and significantly increase its power efficiency beyond that achieved with linear control technology, switch-mode power control techniques are used. All channels are voltage controlled and power is an output variable. Because the lamps are wired in parallel circuits, failure identification techniques prevent the burnout of the second lamp.

Both prior to, and during testing, the parameters for output voltage and its limit level specification are set through the thermal control system's console. This console is also responsible for current channel status and alarm displays, and the measured load current is used to calculate the output power level. The console is connected to eight node controllers and each node controller controls 32 power supplies. These power supplies operate on a closed loop system to provide, regulate, and monitor the specified output voltage. Table 2 lists the operating limits of the thermal control system.

Protection and alarm facilities used by the thermal control system include channel set point level versus monitored level compliance, load detection and shutdown for open- or short-circuits, load-sense line alarms for open- or short-circuits, and out-of-limit alarms. In the event of a municipal power failure, emergency power to the thermal control system is provided by a diesel generator.

Table 2. Operating limits for the thermal control system

NUMBER OF CHANNELS	250, MAXIMUM
LOAD CURRENT / CHANNEL	10 A (DC), MAXIMUM
OUTPUT VOLTAGE / CHANNEL	240 V (DC), MAXIMUM
POWER INPUT	208 V(AC), THREE PHASE 25 KVA
VOLTAGE CONTROL RANGE	0 TO 100 %
PROGRAMMABLE VOLTAGE LEVEL RESOLUTION	1 V DC
SYSTEM CONTROL ACCURACY	LESS THAN 1% OF SET VALUE

## TEST RESULTS

The final infrared absorbed flux results for each IR zone in the MSAT CTV test design are listed in Table 5. The flux values are given for the thermal balance phases only (Phases 1 to 5). Figure 6 is the IRFLUX-generated contour plot for the Phase 3 Nadir IR zone and shows the absorbed flux distribution on the MSAT surface. The predicted radiometer readings, at their actual locations, are highlighted on the contour plots, as seen in Figure 6. For the North and South zones (radiators), additional simulations were performed to reflect the lamp height difference between the radiometer disk and MSAT's surface. More accurate predictions can therefore be used for the radiometer readings. For the East, West and Nadir zones, the radiometer height was not considered. However, the analyses showed that the predictions were not significantly affected by this. Table 3 is an example of radiometer correlations for the Nadir zone during Phase 3.

Table 3. Radiometer correlation for the Nadir zone during Phase 3

NADIR ZONES	PREDICTED MBR FLUXES	TEST RESULTS	ERROR BETWEEN PREDICTIONS AND RELATIVE TEST RESULTS
	(required flux [CLK] is 969.0 w/m <sup>2</sup> )	(required flux [CLK] is 969.0 w/m <sup>2</sup> )	
+ ZOSW (CLK)	962.0	1019.0	0.06
+ ZOSE (CLK)	974.7	973.5	0.00
+ ZOWEST1 (CLK)	972.1	953.1	-0.02
+ ZMWEST2 (CLK)		965.3	-0.01
+ ZOEAST2 (CLK)	975.0	993.4	0.02
+ ZMEAST1 (CLK)		986.9	0.01
+ ZONW (CLK)	964.3	954.1	-0.01
+ ZONE (CLK)	966.3	929.0	-0.01
+ ZMKUW (SUNSHIELD)	525.0	529.5	0.01
+ ZMKUE (SUNSHIELD)	529.9	516.9	-0.02
<b>AVERAGES</b>			
EQUIVALENT MBR AVERAGE (CLK)	970.19	n/a	0.00
EQUIVALENT MBR AVERAGE (SUNSHIELD)	526.95	n/a	-0.01
ZONE AVERAGE (CLK)	968.0	n/a	0.00
ZONE AVERAGE (SUNSHIELD)	524.8	n/a	0.00

For the zones without lamp fluxes, the background radiation was calculated using the radiometer readings without the use of simulation analysis. For the East and West faces, the IR zone was subdivided in three regions, namely: Aft, Forward North, and Forward South. Both Forward regions represent two sides of each dummy feed. The flux uniformity in those regions was greatly affected by the following: the presence of the dummy feeds, the SMA cables, and the L-Band waveguides, as well as the removal of some IR lamps. Although IRFLUX cannot simulate the presence of obstructions inside an IR zone, the flux prediction inaccuracies were less than 10 %.

For the Nadir zone, absorbed fluxes are given for the carbon loaded Kapton blanket surfaces as well as for the Ku-Band antenna's white painted sunshield surface. Also, IRFLUX simulations were performed for both surfaces. The Aft end was subdivided into three regions, namely: the Bus Panel (external to the thrust cylinder), the Thrust Cylinder (inside) and the Plume Shield (white painted surface).

Table 4. IR flux results (W/m<sup>2</sup>) for Phases 1 to 5

ZONE/PHASE	PHASE 1 SPINNING		PHASE 2 WEST SUN		PHASE 3 NADIR SUN		PHASE 4 EAST SUN		PHASE 5 NADIR SUN		
	DATA	REQD	DATA	REQD	DATA	REQD	DATA	REQD	DATA	REQD	
NORTH	245.1	248.0	22.6	n/a	19.3	n/a	144.0	150.0	25.6	n/a	
SOUTH	240.2	248.0	27.8	n/a	21.0	n/a	27.6	n/a	165.7	172.0	
EAST	AFT	345.8	398.0	25.1	n/a	20.1	n/a	1115.5	1152.0	32.6	n/a
	FWD NORTH	320.0	398.0	n/a	n/a	23.8	n/a	617.5	1152.0	36.9	n/a
	FWD SOUTH	235.2	398.0	41.1	n/a	40.1	n/a	883.6	1152.0	57.7	n/a
WEST	AFT	349.6	398.0	1265.0	1286.0	18.0	n/a	27.6	n/a	28.1	n/a
	FWD NORTH	254.8	398.0	689.0	1286.0	17.1	n/a	20.4	n/a	26.4	n/a
	FWD SOUTH	273.0	398.0	1005.8	1286.0	16.0	n/a	18.5	n/a	23.6	n/a
NADIR	MLI	16.1	n/a	15.7	n/a	968.0	969.0	12.6	n/a	1248.3	1259.0
	SUN SHIELD	15.3	n/a	12.7	n/a	524.8	524.0	12.4	n/a	633.0	n/a
AFT	BUS PANEL	18.4	n/a	12.8	n/a	12.3	n/a	15.4	n/a	16.0	n/a
	THRUST CYL.	43.7	n/a	44.5	n/a	39.7	n/a	58.4	n/a	54.1	n/a
	PLUME SHIELD	43.4	n/a	43.4	n/a	38.4	n/a	57.1	n/a	51.3	n/a

Thermal model correlation

To compare the MSAT M2 CTV-1 test results, Hughes Thermal Group had modified the MSAT bulk model and detailed panel models. The MSAT bulk model provided boundary conditions for Hughes Aircraft’s detailed panel models as well as providing predictions for all propulsion systems. Payload and bus unit mounting surface temperatures (UMS) came from four different detailed panel models (North Radiator, South Radiator, Subnadir Panel, and Bus Panel). SPAR provided the temperature gradients from the payload unit to the UMS. Hughes Aircraft HS-601 programs provided the temperature gradients of the bus units.

The correlation used five thermal balance phase results (transfer orbit, on-orbit storage, Equinox BOL no-drive, Summer EOL no drive, and Winter EOL no drive).

Heat pipe conduction in the detailed panel model was verified and validated by the results. In all five thermal balance phases, excellent correlations ( $\Delta t$  less than 3°C) were made for heat pipe temperatures. MSAT’s heater system was dependent on the heat pipes to distribute the heat to the essential units. Heat pipe temperature was a good indicator for radiator temperature distribution. MSAT’s main heat-rejection paths were the North and South Radiator panels. Mounted to the heat pipe equipped radiator panel were all of the high-dissipating Ku-Band and L-Band units. The fixed-conductance heat pipes were primarily used to spread the heat evenly throughout the radiator to help cool down the high-heat-dissipating units and to help maintain the non-dissipating units within an acceptable temperature range.

Hughes Aircraft’s detailed panel model was used to predict UMS temperature. The temperature gradient from an SSPA thermocouple or an LRV to the header pipe was needed to obtain the SSPA temperature for the test correlation. The average temperature gradient was 2.5°C for cold cases, and 2.0°C for hot cases; the  $\Delta t$  would then be used for the post-test correlation of the SSPA.

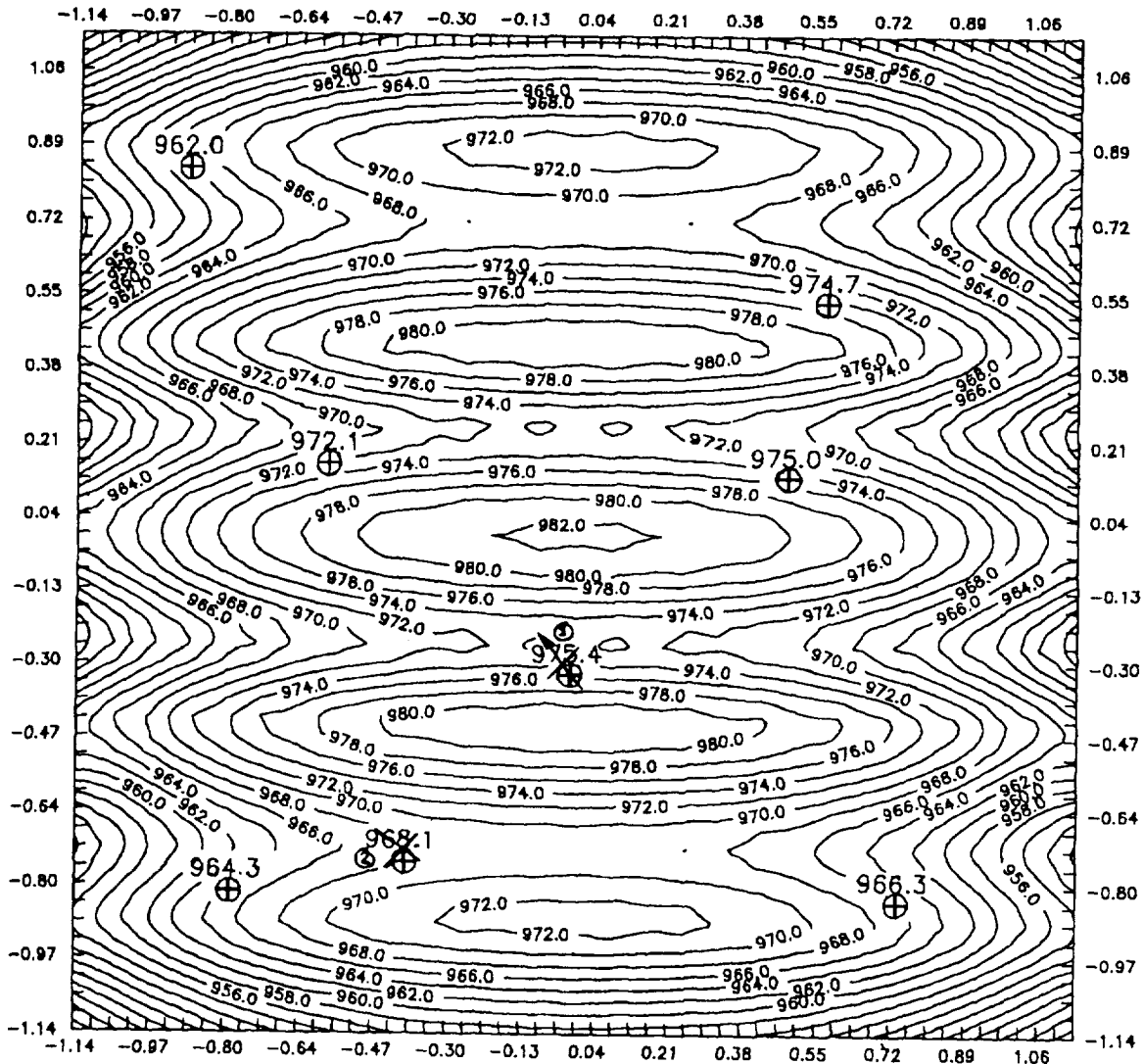


Figure 6. The contour plot generated by the IRFLUX application for the Phase 3 Nadir IR zone

IR lamps supplied heat fluxes to the spacecraft. Radiometers were used to determine the amount of the heat fluxes absorbed by the surfaces. The measured absorbed heat fluxes are listed in Table 4 for each thermal balance phase. Dummy feed temperatures were pre-determined and used as boundaries. The dummy feeds were controlled by the test heaters and adjusted by the E/W IR lamps. Thrust cylinder temperatures were controlled by the test heaters. The MSAT M2 CTV-1 unit predictions and test results are listed in Table 5.

#### Transfer Orbit Thermal Balance (Phase 1)

All payload units were off and the bus and the TT&C units were on. The payload maintenance heaters and replacement heaters were disabled. The spacecraft was assumed to be spinning with a summer sun perpendicular to the spinning axis (Z-axis). The IR lamps were used to apply an orbital average solar heat flux to the East/West blankets and to maintain the North/South exterior radiator temperatures to about 4 °C. The results show that all payload unit temperatures were within 2 °C of predicted values. The propulsion system, TT&C, and the bus units were within the 5 °C range.

Table 5. Thermal balance correlation for three phases

SUB-ASSEMBLY and TV UNIT DESCRIPTIONS	EQUINOX BOL (Phase 3)				SUMMER EOL (Phase 4)				WINTER EOL (Phase 5)			
	ST	PRED	DATA	ΔT	ST	PRED	DATA	ΔT	ST	PRED	DATA	ΔT
<b>SUBNADIR FWD PANEL</b>												
NORTH OUTPUT SWITCH	OFF	1	3	2	OFF	35	35	0	OFF	30	29	-1
NORTH OUTPUT HYBRID MATRIX	OFF	2	2	0	OFF	38	36	-2	OFF	35	33	-2
OHM ISOLATOR TEMP NW	OFF	2	4	2	OFF	43	39	-4	OFF	39	35	-4
OHM ISOLATOR TEMP NE	OFF	8	7	-1	OFF	46	45	-1	OFF	40	39	-1
SOUTH OUTPUT SWITCH	OFF	0	2	2	OFF	25	25	0	OFF	35	36	1
SOUTH OUTPUT HYBRID MATRIX	OFF	1	3	2	OFF	31	31	0	OFF	38	37	-1
OHM ISOLATOR TEMP SW	OFF	0	3	3	OFF	34	35	1	OFF	44	46	2
OHM ISOLATOR TEMP SE	OFF	0	2	2	OFF	36	36	0	OFF	44	45	1
L-BAND RECEIVER	ON	8	8	0	ON	30	29	-1	ON	38	37	-1
KU LOOPBACK FILTER	OFF	0	3	3	OFF	28	28	0	OFF	32	34	2
LO DISTRIBUTION NETWORK	OFF	1	4	3	OFF	26	27	1	OFF	32	34	2
TELEMETRY ENCODER UNIT	ON	8	8	0	OFF	31	31	0	OFF	27	26	-1
<b>SUBNADIR AFT PANEL</b>												
7-FREQUENCY LO	ON	14	13	-1	ON	44	44	0	ON	38	34	-4
2-FREQUENCY LO DOUBLER	ON	9	7	-2	ON	44	43	-1	ON	39	38	-1
COMMAND DECODER UNIT	ON	5	7	2	ON	32	30	-2	ON	35	32	-3
TELEMETRY ENCODER UNIT	OFF	2	5	3	ON	40	39	-1	ON	37	32	-5
<b>BUS PANEL</b>												
IRU	OFF	4	2	-2	OFF	28	28	0	OFF	24	23	-1
MWA	ON	20	21	1	ON	42	41	-1	ON	43	43	0
BDC	ON	9	11	2	ON	35	33	-2	ON	36	32	-4
SCP	ON	14	17	3	ON	38	36	-2	ON	39	36	-3
PDU	ON	8	6	-2	ON	33	31	-2	ON	34	32	-2
VDU	ON	5	4	-1	ON	29	28	-1	ON	29	28	-1
<b>PROPULSION</b>												
LAM INJECTOR	ON	> 3	26	--	ON	> 3	24	--	ON	> 3	38	--
LAM VALVE	ON	> 3	30	--	ON	> 3	43	--	ON	> 3	43	--
OX TANK	ON	3	5	2	ON	31	29	-2	ON	32	30	-2
FUEL TANK	ON	3	5	2	ON	31	32	1	ON	31	29	-2
HE TANK	ON	3	5	2	ON	28	29	1	ON	28	27	-1
<b>NORTH RADIATOR</b>												
SSPA	ON	17	16	-1	ON	46	44	-2	ON	31	28	-3
SSPA ISOLATOR	OFF	3	4	1	OFF	38	36	-2	OFF	24	22	-2
KU RECEIVER	ON	3	3	0	ON	31	29	-2	ON	21	22	1
KU UP-CONVERTER	ON	5	6	1	ON	34	34	0	ON	21	17	-4
KU TWT	ON	26	24	-2	ON	62	57	-5	ON	49	44	-5
KU EPC	ON	4	6	2	ON	33	35	2	ON	22	21	-1
LINEARIZER	ON	2	0	-2	ON	31	33	2	ON	17	19	2
HI-PWR ISOLATOR	ON	0	2	2	ON	39	40	1	ON	25	26	1
TWT R-SWITCH S13	OFF	-4	-2	2	ON	30	29	-1	ON	17	18	1
O/P LPF	OFF	-1	1	2	ON	36	34	-2	ON	23	23	0
RADIO ASTRONOMY FILTER	OFF	-5	-2	3	ON	33	29	-4	ON	20	18	-2
TM TRANSMITTER	ON	7	7	0	ON	33	32	-1	ON	22	20	-2
ULPC	ON	6	7	1	ON	32	32	0	ON	21	20	-1
KU POWER MONITOR	OFF	1	3	2	ON	28	29	1	ON	16	17	1
EXTERNAL LOAD	OFF	2	2	0	OFF	32	31	-1	OFF	23	21	-2
<b>SOUTH RADIATOR</b>												
SSPA	ON	17	16	-1	ON	28	27	-1	ON	47	46	-1
SSPA ISOLATOR	OFF	7	6	-1	OFF	20	18	-2	OFF	34	36	2
L-BAND UP-CONVERTER	ON	11	9	-2	ON	21	18	-3	ON	43	40	-3
COMMAND RECEIVER	ON	3	5	2	ON	15	16	1	ON	34	34	0
TELEMETRY TWT	ON	17	15	-2	ON	43	39	-4	ON	56	53	-3
TELEMETRY EPC	ON	10	12	2	ON	27	25	-2	ON	42	43	1
DC/DC CONVERTER	ON	3	4	1	ON	16	16	0	ON	35	35	0
EXTERNAL LOAD	OFF	3	4	1	OFF	8	10	2	OFF	31	33	2

### On-orbit Storage Thermal Balance (Phase 2)

All the payload units were off and the bus and the TT&C units were on. The payload maintenance heaters and replacement heaters were enabled. The West IR lamps were used. The results show that all payload unit temperatures were within 2 °C. The propulsion system and TT&C units were within the 5 °C range, however some bus unit temperatures were at least 5 °C lower than the predictions. A comparison of the predicted vs. actual bus panel and thrust panel temperatures revealed a discrepancy of 5 °C; this discrepancy was attributed to the fact that the bus panel and thrust cylinder reacted more slowly than the radiators, and had not reached their steady state when the data was taken.

### Equinox BOL No Drive Thermal Balance (Phase 3)

IR lamps were not used. The bus and the TT&C units were on. The payload maintenance heaters were enabled and the replacement heaters were off. The SSPAs and Ku-TWTAs were on at no-drive. The environment was set as a steady state eclipse condition and should be the worst on-orbit cold case. Most units were within the 5 °C range. The 2-frequency local oscillator (LO) and the reference oscillator were 7°C cooler than the predictions. After post-test TC inspection, those TCs used in this Phase were found partially detached.

### Summer EOL No Drive (Phase 4)

East and North IR lamps were used. The bus and the TT&C units were on. The payload maintenance heaters were enabled and the replacement heaters were off. The SSPAs were at no-drive and the Ku-TWTA was at nominal drive. All units were within the 5 °C range. One of the external load in the South radiators was 7 °C cooler than the predictions. After the post-test TC inspection, the external load TC was found partially detached.

### Winter EOL No Drive (Phase 5)

Nadir and South IR lamps were used. The bus and the TT&C units were on. The payload maintenance heaters were enabled and the replacement heaters were off. The SSPAs were at no-drive and the Ku-TWTA was at nominal drive. All units were within the 5°C range.

## CONCLUSION

The stringent test requirements and the high power dissipation of the MSAT payload required the development of versatile IR radiating rigs to accurately simulate required test environments. The IR rig used 122 IR lamps to provide IR heat inputs into six of the seven spacecraft zones. Each zone is contoured with specular reflective baffles to provide < 5 % flux uniformity with a minimum number of lamps. To measure the absorbed flux at 38 spacecraft locations, 49 MBRs were used. The IRFLUX software was used to do simulations and perform post-processing on the six IR zones.

The radiometer test results correlated the software flux prediction and distribution very well. The IR technique developed by SPAR has proven to be an accurate method for correlating the internal thermal network of satellites. An additional advantage is the ability to perform consecutive thermal balance and TV tests. The MSAT bulk and detailed panel models were successfully updated to reflect the thermal balance test results, and the temperature correlations were generally within 2 °C. Four spacecraft tests were conducted with short preparation time and no major problems. DFL proved to be a very reliable test facility and their state-of-the-art equipment and well trained staff supported those tests efficiently.

## REFERENCES

1. S. Samson, P. Theophanous, J. Lemire & M. Donato, "Thermal Test Designs for the MSAT Satellites", 2nd International Symposium, Environmental Testing for Space Programmes, ESTEC, The Netherlands, 1993.
2. C. Ruel, M. Larouche & M. Donato, "Monitored Background Radiometer," 17th ICES Conference, 1987.
3. M. Donato, P. Messidoro & E. Choueiry, "Correlation of the Olympus Thermal Model Using IR Test Data", International Symposium on Environmental Testing for Space Programmes, 1990.
4. M. Donato, J. Green, D. St-Pierre & M. Reeves, "Evaluation of Infrared Test Method for the Olympus Thermal Balance Tests", *The Journal of Environmental Sciences*, 1987.
5. A. Golob, C. Ruel, D. St-Pierre & M. Donato, "Thermal Balance testing of Anik E Spacecraft", 1991
6. C. Ruel & P. Germain, "Error Analysis of the Monitored Background Radiometer", SPAR Report RML-009-88-017, 1988.
7. M. Donato, C. Ruel, A. Harris & B. Muir, "Absorbed Flux Predictions for Spacecraft IR Testing", 14th ICES Conference, 1983.